J. Materials, Conc. Struct., Pavements, JSCE, No.634/V-45, 369-386, 1999 November

3D FEM TOOL FOR PERFORMANCE EVALUATION OF STRENGTHENED RC MEMBERS

Bernhard HAUKE[1] and Koichi MAEKAWA[2]

[1]Member of JSCE, Ph.D., HOCHTIEF IKS (Bockenheimer Landstr, Frankfurt 60323, Germany)

[2]Member of JSCE, Dr. of Eng., Professor, Dept. of Civil Eng., The University of Tokyo (Hongo 7-3-1, Bunkyo-ku, Tokyo 113-8556, Japan)

The aim of this study is to substantiate of a versatile numerical tool for a rational performance evaluation of RC-columns strengthened by steel plate casing or carbon fibre wrappings. Three-dimensional constitutive models of reinforced concrete, carbon fibre sheets, structural steel and steel concrete interfaces to be employed in non-linear finite element analysis of the strengthened column system are formulated. Following the proposed models are verified by full structural analysis of columns subjected to axial, flexural and shear loading conditions. Subsequently, the effectiveness of steel casing and carbon fibre wrappings is studied in view of its mechanism.

Key Words: strengthening, confinement, discontinuities, ductility, finite element analysis

1. INTRODUCTION

After the experience of severe earthquakes in recent years, the need for strengthening RC structures, which were designed years ago, became evident. In order to increase ductility and strength of RC-columns jacketing is a popular method which is commonly used in earthquake zones, and which traditionally uses steel or concrete. Jacketing can also be accomplished by wrapping the column with carbon fibre laminates. Carbon fibre sheets (CFS) are much lighter than steel and are supposed to be used in much smaller amounts due to their high strength. In order to strengthen RC-columns efficiently, as it is necessary to improve strength and ductility and to prevent the catastrophic shear failure, it is imperative to develop tools for rational performance evaluation for the complete system of the strengthened column. Since strengthening material placed around the existing RC-column would provide some state of confinement, the problem is inherently three-dimensional. In this paper, a FEM code for a rational performance evaluation of RC members strengthened by steel plate casing and carbon fibre wrapping is presented.

Many numerical models to determine the cross-sectional strength[1),2)] and structural response[3),4),5)] of concrete filled steel tubes have been proposed. Common simplifications are empirical uni-axial stress-strain models implicitly representing the multi-axial stress strain behaviour of concrete core and steel tube as well as the assumption of perfect bond between concrete and steel. In this study full three-dimensional constitutive models[7), 8), 10)] for concrete and strengthening materials are employed for a rational evaluation of the effect of steel plate casing and CFS-wrapping on RC columns under axial, flexural and shear loading conditions.

The effect of bond properties between steel and concrete columns plays a crucial roll in determining the loading state of steel plates and hence its structural performance. A detailed investigation of the shear transfer mechanism between steel and concrete is beyond the scope of this work and it particularly depends on the actual constitution of the retrofitting system. Then, both extreme cases of perfect shear transfer and no shear transfer are studied first. As such simplifications lead to inaccurate numerical predictions, a softening plasticity steel – concrete interface element based on Carol et al.[12)] is introduced, calibrated with some experimental data and applied to structural analysis of retrofitted systems.

Carbon fibre sheets exhibit very high-tension strength in fibre direction and can be easily applied for strengthening in space-confined areas due to the lightweight nature of the composite. Carbon fibre is much lighter and stronger than steel and only a minimum stiffness increase is added to the column. It is investigated how carbon fibre wrapping

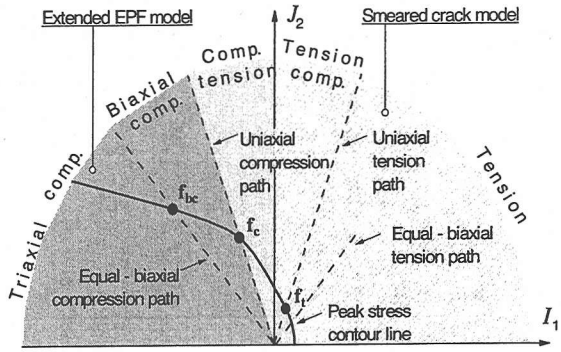

Fig. 1 Generic concrete models in 3D-stress space.

performs in comparison with traditional steel plates as a strengthening material. Finally the strengthening performance comparison has been carried out for these two kinds of materials.

2. MATERIAL MODELS

(1) Reinforced concrete model

By combining the constitutive laws of average stress and average strain for concrete and reinforcement[6], respectively the RC brick element has been constructed[7),8)]. Concrete is, separated by crack initiation, treated in an un-cracked or a cracked concrete routine (**Fig.1**). In the pre-cracking range, the extended triaxial elasto-plastic and fracture model for concrete[9),7)], intrinsically considering the confinement effect on concrete strength and ductility, is employed. After the introduction of cracks, 3D continuity is assumed to be broken and smeared crack modelling of 3D based on in-plane stress-strain relationship of cracked concrete [10] is employed. The crack analysis routine is composed of tension stiffening/softening models across cracks, compression softening model parallel to cracks and shear transfer model along cracks[6]. For reinforcement orthogonal arranged in space distributed representation without dowel shear stiffness has been adopted. Localisation of initial steel plasticity, close to cracks and bond slip effect are considered in computing the mean stress-strain relation based on the local bond-slip behaviour[6].

To consider the different post-cracking behaviour of concrete close and far from reinforcing bars, RC-zoning[11] is used. In the RC-zone, cracking is highly controlled by bond with reinforcement hence stiffening models are employed, while in the plain concrete zone sharp softening is assumed. Considering the directional orientation of bond effect on concrete, RC-zoning is applied in all three directions of an imaginary orthogonal reinforcement system[8], respectively.

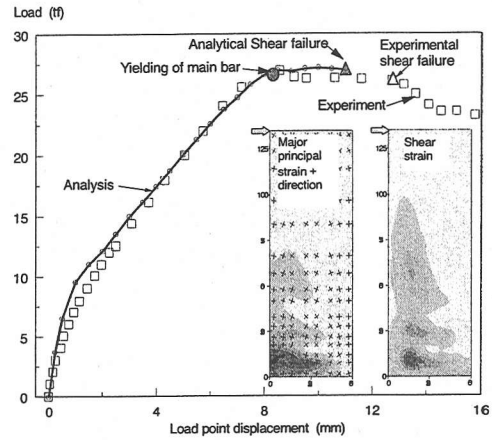

Fig. 2 RC-column: shear failure after yielding of main reinforcement.

For avoiding spurious mesh dependence plain concrete softening is obtained from fracture energy in association with the reference length on which the average softening stress-strain relation of the smeared crack element is determined[7),8)]. The reference length is defined depending on the 3D crack inclination[7),8)].

Stiffening in the RC zone, on the other hand, had been found to be independent of the FE mesh, since cracking would be rather dispersed and propagation would be stable[6]. However, if a control volume contains reinforcement only in one or two directions the average softening/stiffening behaviour depends on the crack inclination relative to the bar. A crack normal to reinforcement will exhibit stiffening due to bond while the other parallel crack would be softening. Consequently, a crack that is neither parallel nor normal to a reinforcing bar but discretionary inclined must show mixed softening/stiffening behaviour. An interpolation scheme based on released fracture energy[8] is employed to define the softening/stiffening behaviour of an arbitrary inclined crack.

A more comprehensive discussion of the three-dimensional RC-model, as well as elaborate verifications can be found elsewhere[8]. Here only two simple examples[8] are presented demonstrating the capability of the RC-model. For the RC-column depicted in **Fig.2** in an experiment after yielding of main reinforcement, sudden shear failure occurred through the progressive propagation of diagonal shear cracks. Analysis closely resembles experimental results. The judgement of shear failure is made in the analysis by a shear strain limit set in the program (set as 1% by default) along the crack direction. From strain distribution at the ultimate step (**Fig.2**), shear failure can be clearly indicated as the computed shear strain suddenly increased over the limit value.

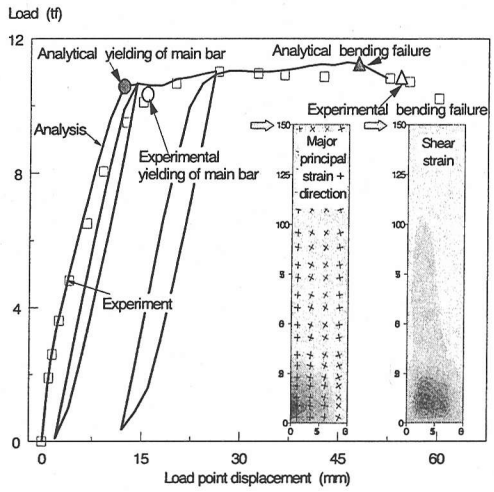

Fig. 3 RC-column: bending failure.

For the slender RC-column, shown in **Fig.3,** failure mode in the experiment was recognised as typical flexural. Observing numerically predicted strain distributions at ultimate and corresponding principal directions (**Fig.3**) damage is found to be localised at the bottom 1/6 of the column height and cracks (principal strain directions) are mostly horizontal. Thus, no indication of shear failure is given and the failure mode can be decided flexural as also observed in the experiment.

(2) Steel plate and carbon fibre sheet models

The steel casing is modelled by quasi-three dimensional layered plate elements considering shear deformations according to the Reissner-Mindlin plate theory. As a layer constitutive model, a parallel elasto-plastic plane stress routine has been implemented.

Carbon fibre sheets are an advanced engineering composite material with very high uni-directional tension strength and a corresponding stiffness similar to steel. Carbon fibre sheets exhibit negligible bending, shear or compression resistance and after it reaches its tensile strength the sheet fails in a perfectly brittle mode. Here, carbon fibre is smeared over the outer brick elements assuming full strain compatibility between carbon fibre and reinforced concrete such that the tensile stress of the carbon fibre can be simply added to the reinforced concrete stress.

3. STEEL CONCRETE INTERFACE

In the numerical analysis of engineering problems, it is often necessary to properly model the behaviour and effect of discontinuities and interfaces. For

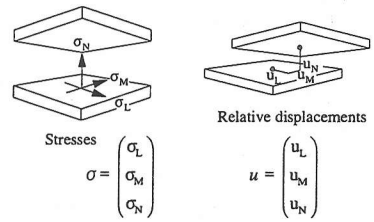

Fig.4 Stresses and relative displacements of the joint-interface element.

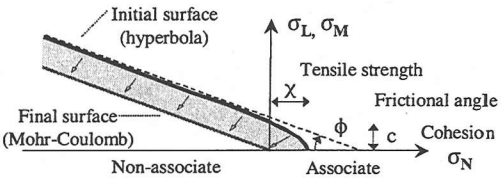

Fig.5 Hyperbolic initial cracking surface and its decay toward a mohr-coulomb frictional criterion.

non-linear analysis of steel-concrete composite, bond slip interface plays a crucial role. This is especially important if no shear connectors such as studs or bolds would be placed such that interfacial shear and normal stress transfer would solely depend on initial bond and friction between steel and concrete. It becomes evident that the common assumption of a rigid connection between steel and concrete would not be reasonable since steel concrete bond strength is easily surpassed by local stresses. Discrete interface elements are well suited to model the discontinuities in case of de-bonding and confinement dependent friction between steel and concrete.

In the present study non-linear interfacial behaviour is described by a softening plastic model which has been originally developed for discrete concrete cracks[12]. In Carol et al.[12] the general formulations and explicit explanations can be found. The entire interface concept is based on the classical stress space theory of plasticity incorporating softening and replacing "yielding" by "cracking" which seems a more suitable term for a de-bonding problem. The basic variables adopted to formulate the model are the three components of the stress vector σ and three components of the relative displacement vector u (**Fig.4**). A three-parameter hyperbolic cracking criterion provides a smooth transition between Mohr-Coulomb frictional criteria at high compression and tension cut off for pure tension (Mode I), given as,

$$f = \sigma_L^2 + \sigma_M^2 - (c - \sigma_N \cdot \tan\phi)^2 + (c - \chi \cdot \tan\phi)^2 = 0 \qquad (1)$$

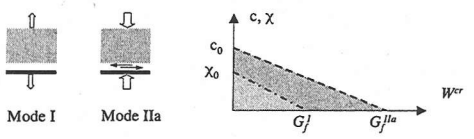

Fig.6 Fracture Modes and softening laws for c and χ.

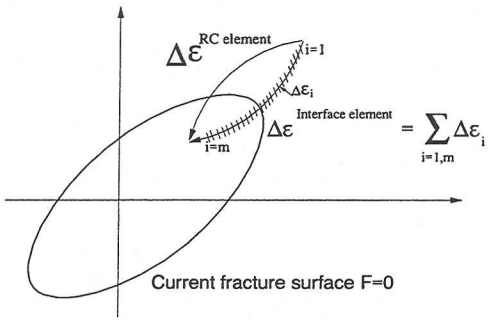

Fig.7 Sub-increments for local interface elements in FEM analysis.

in which tanϕ = frictional angle; c= cohesion and χ =tensile resistance, as shown in **Fig.5**. As bond cracking proceeds the initial cracking surface will shrink. Thereby tanϕ remains constant and the evolution of c and χ is controlled by a single parameter: the work spent on fracture processes during formation of the bond crack, W^{cr}. As W^{cr} increases during fracture processes, c and χ are assumed to soften from their initial values c_0 and χ_0 to zero as shown in **Fig.6**.

In **Fig.6**, G_f^I and G_f^{IIa} are the fracture energies in Modes I and IIa, respectively. Since limited information about softening of steel concrete bond interfaces is known, simple linear softening is assumed (**Fig.6**). By allocating different values for G_f^I and G_f^{IIa} after a complete tension failure of the interface a remaining non-frictional shear resistance, caused e.g. by asperity, can be modelled (**Fig.6**). Under pure tension (Mode I) steel and concrete will completely separate while some surface roughness may remains, which would correspond to another hyperbola passing through the origin (**Fig.5**). In contrast, for confined shearing (Mode IIa), neglecting dilatancy, a final surface of the Mohr-Coulomb criterion (**Fig.5**) will be defined. This corresponds to a solely frictional shear transfer and no tension resistance or, in other words: steel concrete bond is completely broken.

The above-described constitutive model has been implemented in a set of constitutive subroutines for 3D analysis. An elastic-predictor, plastic corrector return mapping algorithm is employed. For convenient numerical integration the finite slip increment is divided into m (m=40~400 in computation) sub-increments that are separately integrated by an explicit 4th order Runge-Kutta scheme (**Fig.7**). After each sub-increment the updated cracking condition (f = 0) is checked to be fulfilled within a given accuracy. Otherwise all data of previously computed sub-increments are discarded, m is increased and integration over the complete increment repeated.

In order to demonstrate the basic features of the model two purely numerical examples at constitutive level are presented, showing the varying shear strength for constant pre-imposed tension or compression loading. In a first load step a certain amount of tensile or compressive stress, respectively is applied (σ_N = 0, 20, 60 kgf/cm^2; σ_N = 0, -20, -60 kgf/cm^2).

Then, the shear relative displacement is increased progressively keeping the normal stress level constant. Results are depicted in **Fig.7** for shear/tension and **Fig.8** for shear/compression. As expected, the pre-imposed tension load reduces while confinement increases the available shear resistance. For shear/compression (**Fig.8**) all descending curves show a first steep part where both softening parameters c and χ decrease and ultimately all curves tend toward a residual value of shear stress, which is governed by the frictional law.

The ability of the interface model has been shortly demonstrated at a constitutive level. In a following step the constitutive law is implemented into the FE code COM3 utilising a 16-node isoparametric interface element of zero thickness. Then, taking a simple example, the consistency of the implementation and the appropriate updating of the path dependent parameters in the context of global equilibrium iteration shall be proven. For this purpose a simple pullout test of a steel plate embedded in concrete had been chosen. In **Fig.9** the lay out of the specimen[13] and the 3D finite element discretization is shown. Material parameters are used according to Gao et al. [13] as c_0=7.1kgf/cm^2 and G_f^{IIa} = 0.6kgf/cm^2 or assumed as χ_0=7.1kgf/cm^2, G_f^I =0.2kgf/cm^2 and tanϕ =0.8. According to Geo's numerical result by trial and error, the initial elastic shear stiffness is set as K=15000 kgf/cm^2.

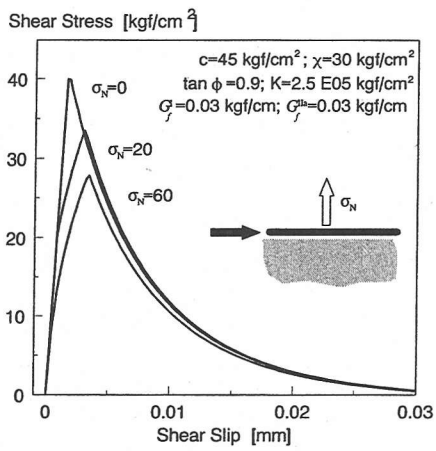

Fig.8-1 Shearing under constant tension.

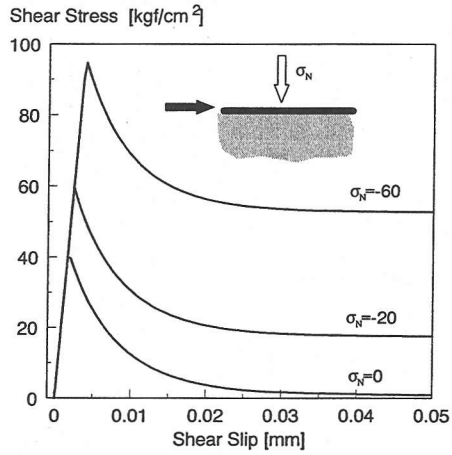

Fig.8-2 Shearing under constant confinement.

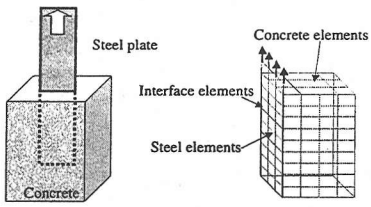

Fig.9 Pull-out specimen and FE-discretisation.

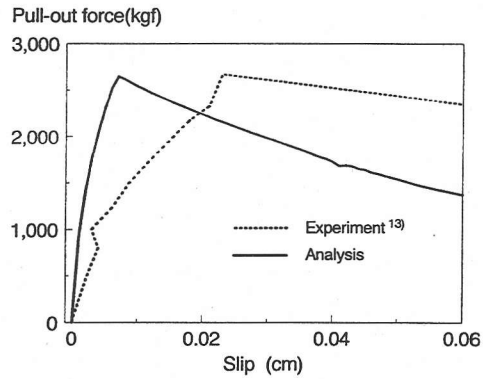

Fig.10 Pullout force vs. slip.

Fig.10 compares computed and experimentally obtained pullout force – slip diagram. Although the capacity and the slope of descending branch seem fairly well, the stiffness up to the peak differs considerably. It is easy to adjust the analytical result in using the shear elasticity different from the original reported value. But, the mere play with values might be meaningless in considering that the initial steel-concrete bond before softening slip will be notably affected by shrinkage, moisture content, irregularity of steel plates, etc. For a part of the analytical tool to represent strengthened RC, the authors decided to adopt Carol's model covering the capacity and post-peak response with friction.

4. CONFINEMENT EFFECTIVENESS

(1) Effect of steel - concrete shear transfer mechanism

The elasto-plastic and continuum fracture (EPF) model of confined concrete[9] has been successfully used for the analyses of discretely hoop confined concrete columns subjected to axial compression[14].

In this case lateral steel acts solely in circumferential direction and naturally does not directly contribute to the axial load bearing mechanism. Steel encasement, on the contrary, adds not only lateral but also axial strength and stiffness to a concrete column. In that case the shear transfer mechanism between concrete and steel plays a crucial role in determining the loading state of steel plates. The most effective confinement must be expected if there was no shear transfer such that the casing could act as pure confining agent similar to dense arranged lateral hoop reinforcement. The assumed, in contrast, is a perfect shear transfer mechanism between steel encasement and concrete core would lead to a biaxial stress state in the steel plate. In that case, the capacity of steel jacketed to confine the concrete core, would depend largely on the amount of axial stress resisted by the steel plate.

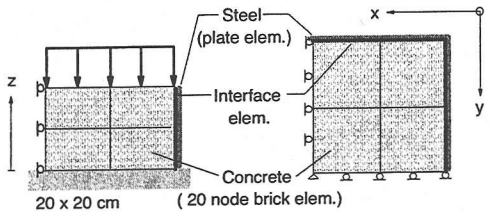

Fig.11 FE discretisation of steel plate confined concrete column (sectional analysis).

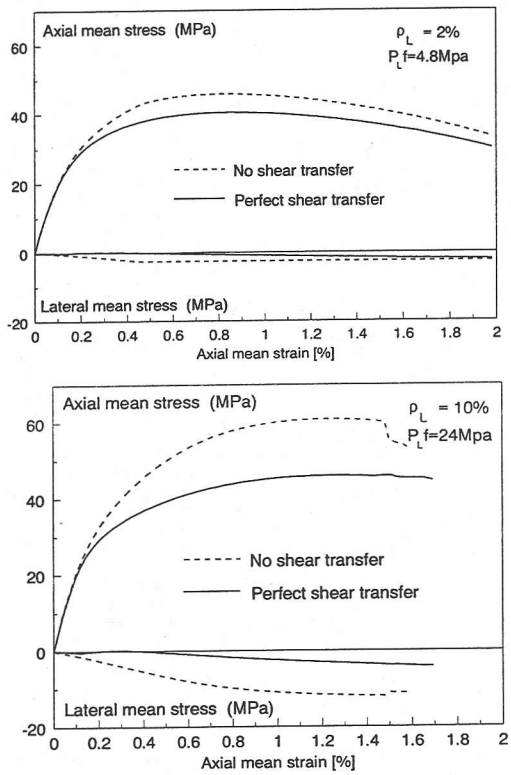

Fig.12 Steel confined compression: effect of shear transfer mechanism on confinement effectiveness of steel casing.

By means of non-linear three-dimensional finite element program COM3, the sectional average axial and lateral stress-strain relationship of confined concrete of unit-length steel encased concrete columns is determined. As for axial compression reinforcing bars are neglected, only concrete and confining agent are considered. A 20-cm square section is studied specifying concrete cylinder strength $f_c' = 400$ kgf/cm^2 and steel yield strength $f_y = 2400$ kgf/cm^2. For making use of symmetry, one quarter of the section is taken as finite element domain using four concrete brick elements for the section and two over the height (**Fig.11**). Steel encasement is modelled in computation by plate elements. For discrete interface elements placed between steel and concrete either perfect or no shear transfer mechanism is assumed (**Fig.11**).

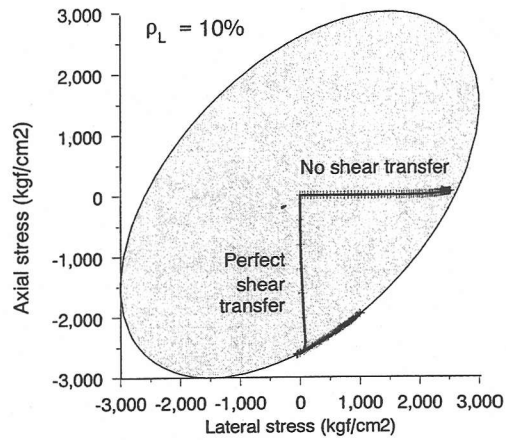

Fig.13 Axial vs. lateral steel stress history in the von Mises plane stress yield locus.

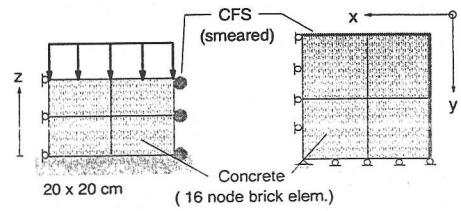

Fig.14 FE discretization of CFS confined concrete column (sectional analysis).

The following stress-based parameters, called volumetric averaging of the axial mean stress $\overline{\sigma}_A$ and the lateral mean stress of concrete $\overline{\sigma}_L$ are introduced as [14],

$$\overline{\sigma}_A = \frac{1}{V_c}\int_{V_c} \sigma_{c,zz}(x,y,z)\,dV \qquad (2)$$

$$\overline{\sigma}_L = \frac{1}{V_c}\int_{V_c} \frac{\sigma_{c,xx}(x,y,z) + \sigma_{c,yy}(x,y,z)}{2}\,dV \qquad (3)$$

where $\sigma_{c,ij}$ is defined as concrete stress tensor and V_c is the analysed domain of concrete (see **Fig.11**). The volumetric averaging of lateral mean stress $\overline{\sigma}_L$ expresses the entire confinement supplied by the lateral confining agent and is regarded as mean confinement index. In **Fig.12** computed mean axial and lateral concrete stress versus axial strain for 2% and 10% lateral reinforcement ratio are shown. It becomes clear that the peak strength of confined concrete must be dependent on the steel concrete interface shear transfer mechanism. If we specify the shear transfer to be negligible, average confining stress and corresponding axial stress at peak is much higher than that of the perfect shear transfer case.

The possible confining capability of steel or CFS, is defined as available confinement potential, $\rho_L f$ [16] with ρ_L as the volumetric ratio of lateral steel/CFS

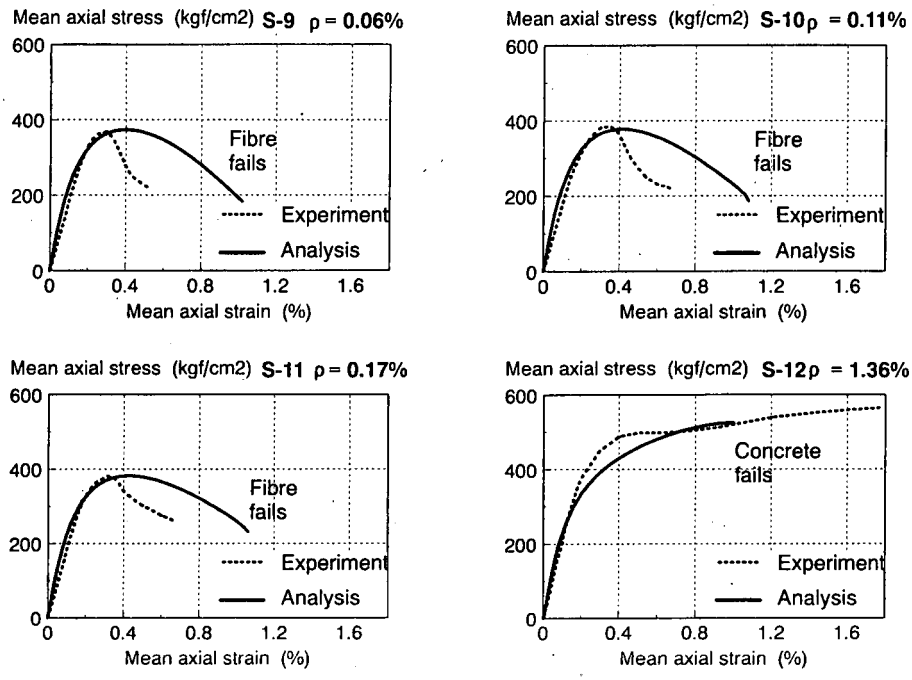

Fig.15 Average axial concrete stress strain diagrams.

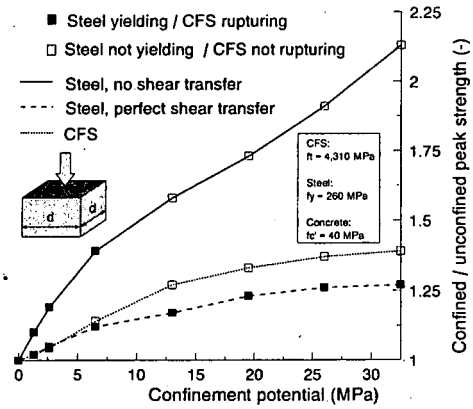

Fig.16 Peak strength vs. confinement potential.

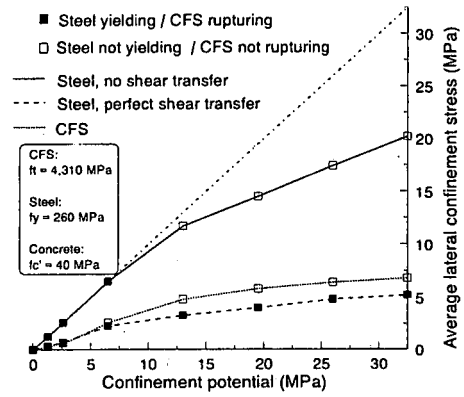

Fig.17 Actual induced vs. available confinement.

and f as the yield strength (steel) or tensile strength (CFS) of the confining agent. It describes the maximum available confinement capacity lateral confinement can induce on concrete and must be in equilibrium with mean concrete lateral stress. The closer the actual induced lateral (confinement) stress level would be to the available confinement potential the more effective use is made of the confining agent[16].

To improve the understanding of how the steel encasement contributes to lateral confinement and axial load carrying during the load history average axial steel stress is plotted versus average lateral stress (**Fig.13**). The von Mises yield locus under plane stress conditions, which was assumed in computations, is also depicted in **Fig.13**, neglecting small shear stresses in drawing the ellipses. Because of no shear transfer, assumed the stress point stays close to the abscise, reflecting nearly uni-axial stress state, and yielding occurs under lateral stresses. Almost no axial stress is observed throughout the loading history. On the other hand, if perfect shear transfer is specified, the stress point moves first quickly along the ordinate and steel yields under axial stresses. With further loading the stress point transits along the yield locus such that axial stress level reduces and some confinement effective lateral stress can build up.

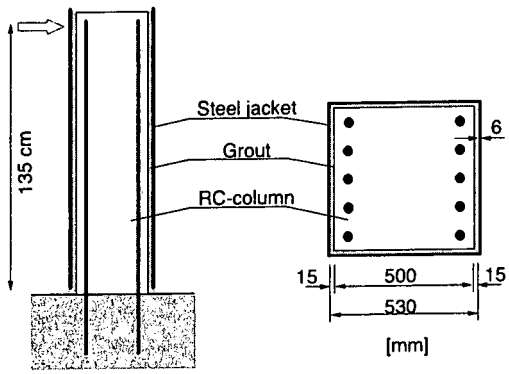

Fig.18 RC-column strengthened by steel casing [19].

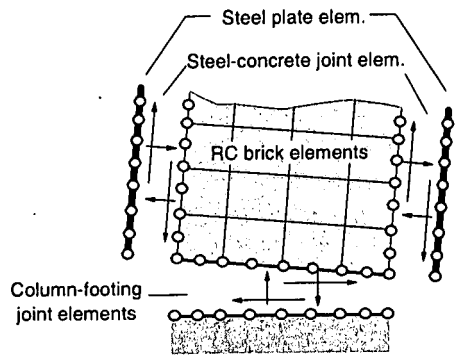

Fig.19 Discontinuities in FE-discretization (2D view).

(2) Carbon fibre sheets as confining agents

Carbon fibre sheets (CFS) are nowadays becoming popular as strengthening material for existing reinforced concrete columns. For axially loaded columns, CFS wrapping may provide some lateral confinement to the concrete column increasing its compressive strength and ductility. By employing the EPF-model for confined concrete[9], the confinement effect of CFS wrapping on axially loaded concrete columns is numerically investigated. Finite element discretization of a 20-cm square section concrete column is similar as described in the previous section for steel confined concrete. Carbon fibre sheet is smeared over the outer brick elements assuming full strain compatibility between carbon fibre and reinforced concrete (**Fig.14**).

In **Fig.15** analytical and experimental[15] average stress-strain relationship for CFS confined concrete is given. Concrete cylinder strength for all specimen was specified as f_c'=384 kgf/cm^2 and unconfined compressive strength of the column was numerically obtained as 371 kgf/cm^2. For low lateral reinforcement ratios (S-9 – S-11), the confinement effect is very small and specimen failure is caused by rupture of the CFS. Only for a high lateral reinforcement ratio remarkable strength improvement can be achieved and the failure mode is changed from fibre rupture to concrete compression failure (S-12). This tendency can be fairly grasped by numerical analysis (**Fig.15**). On the other hand, average axial concrete strain, as obtained experimentally, does not agree well with numerical results, especially in the post-peak regime. The EPF-model for confined concrete was derived for 20 cm high test specimens[9], but tested CFS-confined columns[15] were 60 cm high. Then, considering the localisation of post-peak compression fracture, it seems to be reasonable that experimentally obtained descending branch is much steeper than in analysis.

(3) Confinement performance: CFS-wrapping versus steel-casing

In the previous sections performance of steel casing and CFS wrapping as confining agent for retrofitting concrete columns has been studied. Now confinement efficiency of steel and CFS is to be compared. As a rule of thumb, one can say that CFS exhibits a rupture strength, which is about ten times higher than the yield strength of commonly used structural steel, while Young's modulus is approximately the same. Consequently, it could be argued that only one-tenth the material amount of CFS would suffice to achieve the same structural performance as steel. Confining concrete actually means restricting its expansion. Then, the point of interest is whether the reduced amount of CFS, having the same failure load as steel but much higher elongation, could be effectively used confining concrete expansion.

To obtain systematic information peak axial and lateral stresses were computed for different confinement potentials using sectional analysis as previously introduced. Normalised axial peak strength in **Fig.16** and corresponding confining stress in **Fig.17** are plotted versus the confinement potential. Steel jacketing with no shear transfer always outperforms CFS wrapping as a pure confining agent. Carbon fibre provides only corner confinement, while steel introduces corner and bending confinement on concrete core[16]. Through its higher axial and additional bending stiffness, steel allows a much slower expansion of concrete core than CFS does and hence provides higher actual lateral confining pressure. However, if steel does not solely provide lateral confinement but also sustains axial load its confining efficiency reduces so much. In the case of full shear transfer the confining performance of CFS surpasses that of steel. It should be noted that if steel does not yield or fibre does not rupture, the ratio of induced and

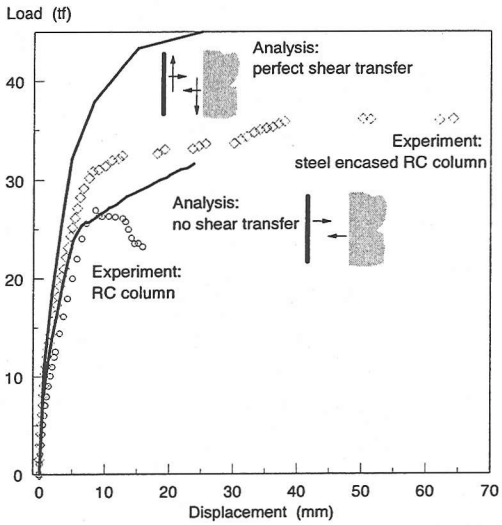

Fig.20 Influence of steel-concrete shear transfer mechanism.

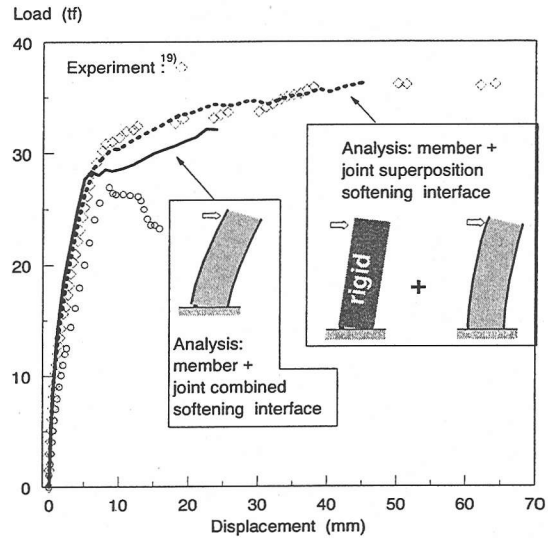

Fig.21 Combined and separated analysis of member and joint response: steel encased RC-column.

potential confinement decreases remarkably and the strength gain becomes smaller (**Fig.16**). Although carbon fibre exhibits a very high-tension strength, due to a Young's modulus similar to that of steel, the confining effect generally remains lower. The higher strength of CFS cannot be fully exploited except in the case of very large deformation occurring in the RC members.

5. STRENGTHENING BY STEEL CASING

Most analytical and/or experimental studies of steel encased concrete or reinforced concrete columns found in literature, deal with new structures. In that case, the composite column is constructed using a hollow steel section as concrete formwork guarantying an inherent shear transfer mechanism between steel end concrete through bond and friction[17), 18), 5)]. If, on the other hand, an existing RC-column is post-strengthened by means of steel encasement a gap between concrete member and steel jacketed is unavoidable and needs to be grouted, usually by non-shrinkage mortar[19)]. Then, steel-concrete shear and normal stress transfer mechanism becomes even more complex than that for concrete filled hollow sections. Furthermore, at the bottom of the column (critical section) only RC-specimen provides direct resistance contribution. Steel casing is discontinuous at the bottom section (**Fig.18**) and hence can only provide confinement on the RC core. Another possibility would be to anchor the casing to the footing thus ensuring continuity. In that way, strength of the column can be largely enhanced. However, existing substructure, such as pile cap and piles are usually not designed to support such increased loads and may be difficult to strengthen. Then, this kind of strengthening system is not considered here.

(1) Consideration of discontinuities in analysis

The actual shear transfer between steel casing and RC-specimen is very complex and not well understood. However, assumption of perfect strain compatibility as commonly used for analysis of steel concrete composite structures may not be appropriate. As a trial, perfect shear transfer and no shear transfer, respectively are assumed in analysis. As results are depicted in **Fig.20** it becomes unequivocal that assumption of perfect shear transfer in no case yields realistic results, but a bold overestimation of strength and stiffness. On the other hand, if no shear transfer would be specified in analysis for steel concrete interface, initial stiffness is only slightly below experimental results[19)] (**Fig.20**) indicating that there is no significant relative displacement between steel and concrete at the early loading stage. However, yield level and ductility are clearly below experimental results, which might be due to the absence of any steel-concrete shear transfer. It is evident that no shear transfer is a very conservative assumption. For more realistic estimations of the entire column system response softening steel-concrete stress transfer model seems to be desirable since simplified assumptions of shear transfer mechanism proved to be less accurate as demonstrated.

Using softening plasticity discrete interface model, as above described, may be one way of considering relative displacements between reinforced concrete core and steel jacket and corresponding stress transfer in a consistent manner. The only problem arising is the proper definition of steel-concrete interface material parameters. Values of shear bond strength (parameter c_0 in softening plasticity model) found in literature[17), 5), 13)] range from as low as 2.0 kgf/cm^2 up to about 10.0 kgf/cm^2 with the actual value largely scattered. For corresponding opening bond strength (parameter χ_0), no values are found in the literature and hence the same value as shear bond strength is used for simplicity. For shear fracture energy (parameter G_f^{IIa}) values between 0.4 and 0.6 kgf/cm had been proposed[13)] which were obtained from pull out tests. Opening mode fracture energy (parameter G_f^I) is assumed between 0.1 and 0.2 kgf/cm. Elastic stiffness (parameter K) is assumed as the same for shear and opening modes and taken between $1.5x10^4$ and $2.5x10^4$ kgf/cm^2 [13)]. Frictional angle (parameter tanϕ) for steel-concrete interfaces is commonly assumed as 0.8.[20)]. Nil compression-shearing dilatancy for the smooth steel-concrete interface is assumed.

All above described parameters had been derived for direct steel-concrete interface through push or pull out tests. In the present case of a post-strengthened RC-column we also have the mortar-grout interlayer between steel and concrete (**Fig.18**) and no information is available how it would influence the interfacial behaviour. However, since all parameters have a clear physical meaning, an "educated guess" can be made. Then, by comparing analytical and experimental results the choice of parameters can be improved. Proceeding like this, finally a set of parameters was decided (c_0=8.0 kgf/cm^2, χ_0=8.0 kgf/cm^2, tan ϕ=0.8., G_f^I = 0.2 kgf/cm^2, G_f^{IIa} = 0.6 kgf/cm^2, K=$1.5x10^4$ kgf/cm^2). It was found that variations around this set do not lead to significant alterations of numerical results.

With above parameters for steel-concrete joint, RC parameters left unchanged as successfully used for the bare RC specimen (**Fig.20**) and steel casing characterised by yield strength and Young's modulus[19)], strengthened column is analysed. First, column-footing joint[6)] is allocated and the pull out effect is analysed together with member response (**Fig.21**). It is anticipated that stress release at the joint location would lead to some reduction of 3D confinement at the bottom section and hence influence the over all response. Computed response generally agrees with experimental data up to the onset of reinforcement yielding (**Fig.21**) indirectly verifying the choice of interfacial parameters.

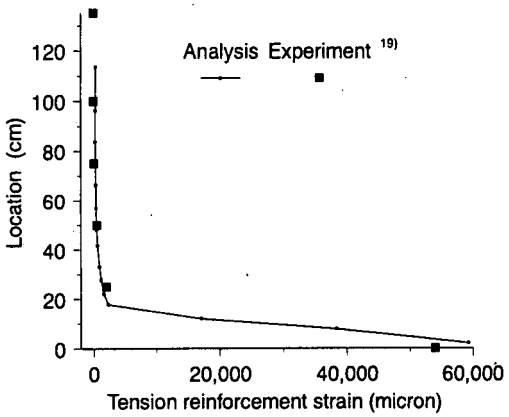

Fig.22 Tension-side steel strain distribution at failure.

In an attempt to overcome the numerical instability problem, joint and member analysis are separated. It is recognised that combined analysis of joint and member response of steel encased RC-columns constitutes a three-dimensional numerical problem of high complexity calling for further improvements of computational stability for simulating structural response up to the ductility limit.

Column-footing joint response is analysed using a rigid column by allocating elastic brick elements with the highest stiffness. Member rooted displacement is independently determined ignoring column-footing joint response. Finally, joint and member response are superimposed (**Fig.21**). So the obtained load displacement diagram is close to previous combined analysis for pre-yielding response, supporting the validity of separate analysis and subsequent superposition. Furthermore, separate analysis enables computation to proceed behind yielding point up to ductility limit. Fair agreement with experimental results can be noticed (**Fig.21**). As could be expected, combined member + joint analysis results in a perceptibly lower yield level than for separate analysis because of joint-member interactive effects. As joint opening increases confinement effect at the bottom of the column decreases reducing the computed strength gain.

As a further solidification of the analysis scheme numerically derived tension-side reinforcement strain distribution at failure is compared with experimentally obtained data[19)]. Experimental strain distribution (**Fig.22**) reflects the average of several strain gauges attached to different reinforcing bars at the respective specimen heights. For the bottom most positions, however, only one intact gauge was left. It is very interesting to notice that for the steel encased RC-column very high strain values can be reached in tension reinforcement. Any bare RC-

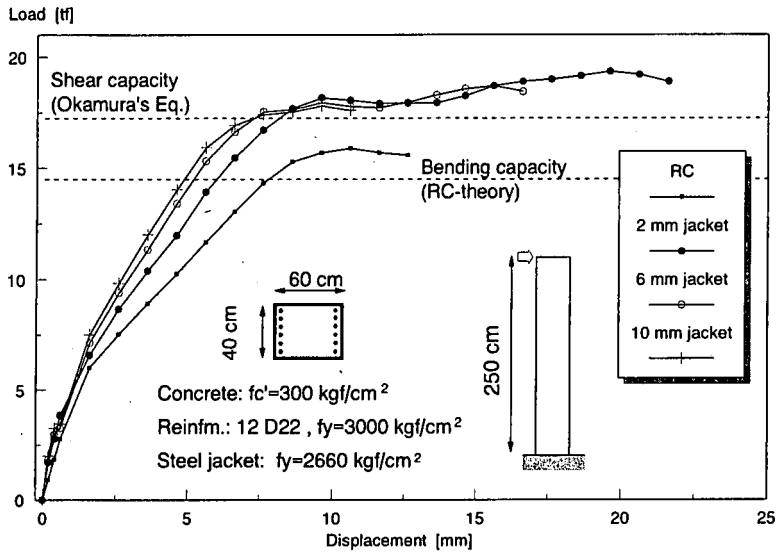

Fig.23 RC-column failing in flexure strengthened by steel casing.

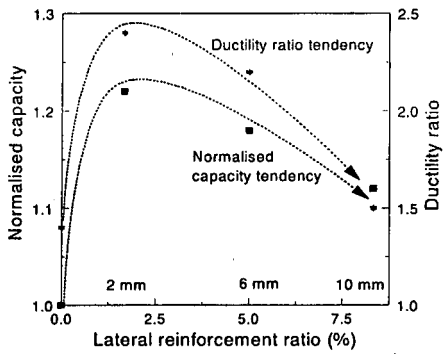

Fig.24 Computational ductility and capacity for flexure failing RC-column strengthened by different quantities of steel casing.

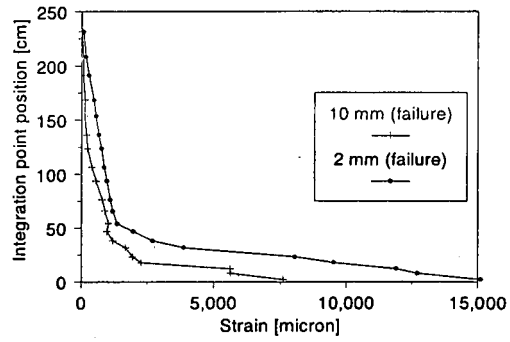

Fig.25 Flexure failing RC-column post-strengthened by low (t=2mm) and high (t=10mm) quantity.

column would already have collapsed due to concrete compression failure, reinforcement buckling or/and spalling of concrete cover before such large steel strain values could develop. However, for steel encased RC-columns concrete strength and ductility is so much enhanced due to confinement induced by the steel jacketed. Then, it also becomes imperative to correctly model tension reinforcement constitutive law up to the ultimate [8].

(2) Effectiveness of steel jacketing with varying plate thickness

One of the major points of interest when planning and designing post-strengthening of RC-columns by means of steel casing is the question of how much steel shall be placed for effective retrofitting.

Generally, there are a number of constraints for the steel plate thickness in terms of availability or feasibility of the retrofitting process. If, for example, steel plates were too thin they would easily buckle causing severe difficulties during transport and construction work. Very thick plates, on the other hand, may be hard to handle because of its inherent weight or be difficult to weld. However, only aspects of structural performance are discussed here.

First, an RC-column failing in bending, as depicted in **Fig.23**, is studied. Bending capacity of the bare RC-column, computed according to RC-theory, is lower then shear strength predicted by Okamura's empirical equation[21]. For numerical analysis of the steel encased column, the same steel-concrete interface parameters are used as introduced and substantiated before. Adding 2, 6 or 10 mm thick steel jacket to the RC-column can increase capacity and ductility. The more lateral steel that is provided the stiffer the pre-yielding response (**Fig.23**), which seems logic. However, obviously an inverse relationship between lateral steel plate reinforcement ratio and flexural performance exists.

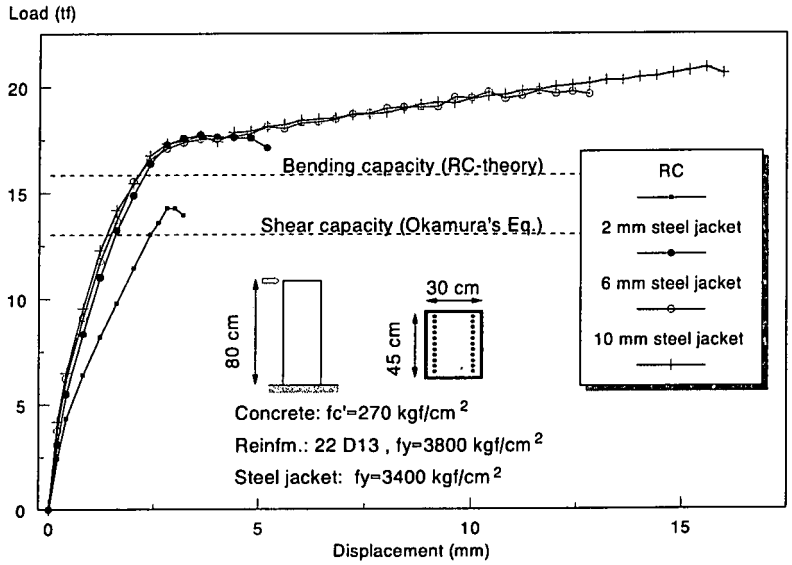

Fig.26 RC-column failing in shear strengthened by steel casing.

Table 1 Computational displacement and ductility ratio.

Steel casing	δ_y	δ_{max}	μ
2mm	9.0	21.6	2.4
6mm	7.5	16.6	2.2
10mm	7.01	10.6	1.5

As we plot moment capacity of the strengthened column system normalised by bare RC-column moment capacity over lateral steel plate reinforcement ratio (**Fig.24**), it becomes evident: the more lateral steel that is provided the less capacity improvement can be achieved. Similar conclusion can be reached by comparing the ductility ratio. The definition of ductility in this paper is: $\mu=\delta_{max}/\delta_y$, where δ_{max} is the displacement corresponding to the maximum load and δ_y is the displacement corresponding to the yielding load. These displacements and calculated ductility ratio are shown in **Table 1**.

From **Table 1** and **Fig.24**, we can find a thin steel jacketed results in high ductility whilst a thicker one reduces ductility coming close to the un-strengthened column's value for the 10 mm steel casing (**Fig.24**).

Any increase of lateral displacement after main reinforcement yielding of a slender RC-column will result in an almost constant resistance force. Further strength gain is usually only caused by strain hardening of reinforcing bars under large deformations. Then, in order to allow the column to experience such high lateral displacement without structural failure and thus gaining capacity enhancement due to strain hardening, a large rotational capacity is necessary. For rotational capacity the additional axial stiffness of the steel casing might be contra-productive. Then, possible capacity improvement due to lateral confinement is contradicted by a reduced rotational capacity caused by the added axial stiffness.

As an indicator of curvature and hence rotational capacity, steel strain distribution of the analysed columns is taken (**Fig.25**). For 10 mm steel casing failure occurred already when steel strain is mostly localised at the bottom 20 cm of the column, thus rotational capacity remains small. For only 2 mm steel casing, on the other hand, large steel strain can spread up to about 50 cm height of the column upon failure and hence guarantying much larger rotation of the column. It can be concluded that when strengthening RC-columns failing in flexure, by steel encasement, special attention must be taken to maintain the rotational capacity. From that point of view it seems that the thinner the steel jacket that can be provided the more effective it is, or in other words: "less is more".

Following, another RC-column, failing in shear, is studied (**Fig.26**). This time bending capacity is kept intentionally well above shear capacity in order to provoke the brittle shear failure for the bare RC-column (**Fig.26**). Again, steel jackets of different thickness (2, 6 or 10 mm) is allocated in analysis for the purpose of numerical evaluation of the changed strengthening effect. Steel-concrete interface parameters are taken as previously used. For RC-columns failing in shear, a direct relation between the amount of attached steel and strength or ductility gain can be observed (**Fig.26**). This is quite contrary to the above conclusion for retrofitting of columns with sufficient shear capacity failing in bending

Table 2 Computational displacement and ductility ratio.

Steel casing	δ_y	δ_{max}	μ
2mm	2.8	4.8	1.7
6mm	2.8	12.8	4.57
10mm	2.8	15.6	5.57

(**Fig.23**). For the present case, however, as shear resistance of the un-strengthened column is inadequate, steel encasement is primarily put to use as extra shear reinforcement. Then, the more lateral steel is provided the more shear resistance might be improved and ultimately failure mode may be changed toward flexure such that higher ductility can be enjoyed. A similar calculation has been done for ductility ratio (**Table 2**). As we plot normalised capacity and ductility ratio over lateral steel plate reinforcement ratio (**Fig.27**) it is manifested that an increase of lateral steel provided is followed by capacity and ductility improvements.

In **Fig.28,** steel strain distribution of tension side reinforcement of strengthened column is displayed. For a 2.0 mm steel jacket shear failure had occurred already when only some mild strain localisation at the bottom of the column could take place. For a 10 mm steel jacket, on the other hand, large steel strain can develop up to about 1/5 of the height of the column upon failure indicating the change of failure mode from brittle shear to ductile flexure.

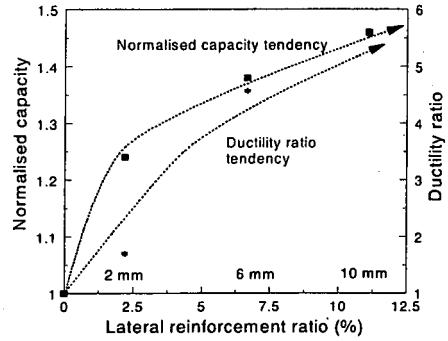

Fig.27 Computational ductility and capacity for shear failing RC-column strengthened by different quantities of steel casing.

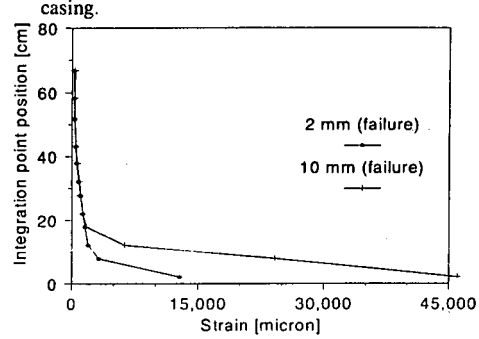

Fig.28 Shear failing RC-column post-strengthened by low (t=2mm) and high (t=10mm) quantity of steel casing: steel strain distribution at failure.

6. STRENGTHENING BY CFS WRAPPING

In a previous section carbon fibre sheets (CFS) had been employed as confining agents for axially loaded concrete columns. In this section CFS-wrapped RC-columns subjected to lateral and axial loading are studied. In order to employ CRS wrapping for efficiently strengthening of reinforced concrete columns, it is indispensable to establish up to what extent encasement with CFS improves ductility and strength of existing reinforced concrete columns.

(1) RC-columns failing in flexure

In **Fig.29** an RC-column is shown which had been tested[22] using varying quantities of CFS-wrappings (non, 1 layer ≅ 0.05%, 2 layers ≅ 0.1%). First, an axial load of 8 tf was applied followed by displacement controlled lateral loading. Un-reinforced RC-column ST-N fails in flexure with a ductility ratio of about four (**Fig.29a**). Adding of one or two layers of fibre wrapping, respectively improves ductility ratio up to seven and brings a slight strength increase (**Fig.29a**).

Finite element analysis (**Fig.29b**) can grasp experimental response up to ultimate load level fairly well. Improvements of ultimate strength and corresponding ductility are nicely predicted. Only the gently descending branch of the fibre wrapped specimens, which is associated with remarkable residual strength, cannot be fully reflected. From **Fig.30** it can be clearly observed that CFS-wrapping of RC-columns failing in flexure leads to an increased ductility rather then strength gain of the retrofitted system. It can be understood that the relatively lower stiffness of CFS causes less effectiveness of confinement at smaller deformation of RC and the large straining of some part of members can just extract the CFS high performance.

(2) RC-columns failing in shear

It had been shown that carbon fibre wrapping could improve flexural ductility and capacity. In that case CFS-wrapping is mostly utilised as a concrete confiner. On the other hand, if failure of the un-strengthened column is caused by brittle shear mode CFS-wrapping primary acts as additional shear reinforcement. Then, the aim of strengthening should be the preventing of shear failure such that a more ductile flexural mode could be enjoyed.

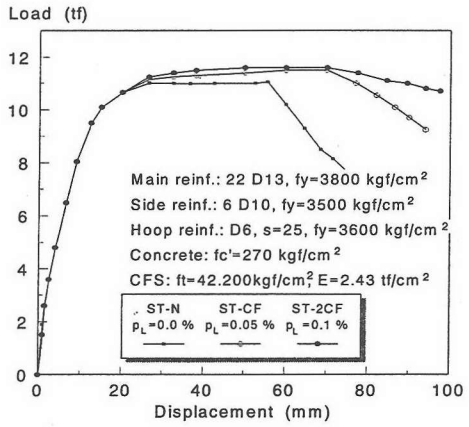

a) Envelopes of reversed cyclic experiments (Osada et al. 1997)

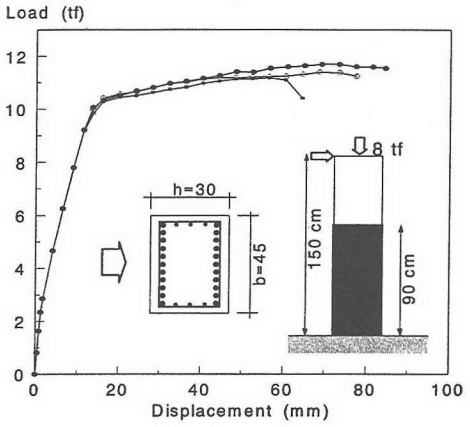

b) monotonic analysis

Fig.29 CFS-wrapped RC-column failing in flexure Envelopes of reversed cyclic.

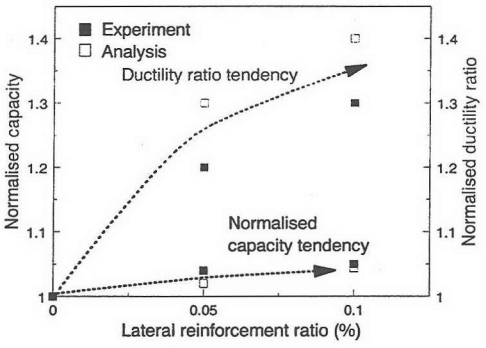

Fig.30 Flexure failing RC-column strengthened CFS-wrapping: capacity and ductility improvements.

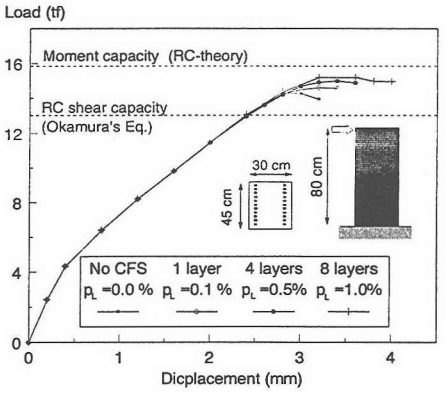

Fig.31 Shear failing RC-column strengthened by CFS wrapping: analysis.

In order to provoke shear failure above analysed RC-column failing in flexure (**Fig.29**) is modified reducing its height to 80 cm and omitting side reinforcement and hoops. Other parameters are left unaltered. Only lateral loading was applied to the specimens. Analytical results are depicted in **Fig.31**. As could be expected, bare RC-specimen suddenly fails in shear. As one, four or eight layers of carbon fibre sheets are attached to the specimen shear failure still cannot be prevented but predicted failure mode becomes more ductile. For specimens with four or eight layers of CFS, it may be expected that a substantial residual strength is remaining, which cannot be reflected by computation. However, it should be noted that whatever layers of CFS would be provided, shear failure took place closer to the yielding point of reinforcement, CFS-wrapping seems less effective for strengthening shear failing RC-columns. The shear strengthening due to CFS is not so obvious because shear deformation is not large enough to bring into full capacity of confining performance.

7. EFFECTIVENESS OF STRENGTHENING

In this chapter, mechanics oriented discussion on the effectiveness of strengthening by steel and CFS having quite different characteristics is aimed. Here, the authors intend to clarify the mechanics of strengthening in terms of failure modes of the target body of RC columns to be strengthened. Of course, the engineering judgement and selection of construction system for retrofitting are performed in consideration of multiple factors such as merits and shortcomings in cost performance and period of construction. This chapter is not directed to the engineering efficiency of retrofitting methods but only addressed to the mechanical view of steel and CFS-wrapping attached to the targets.

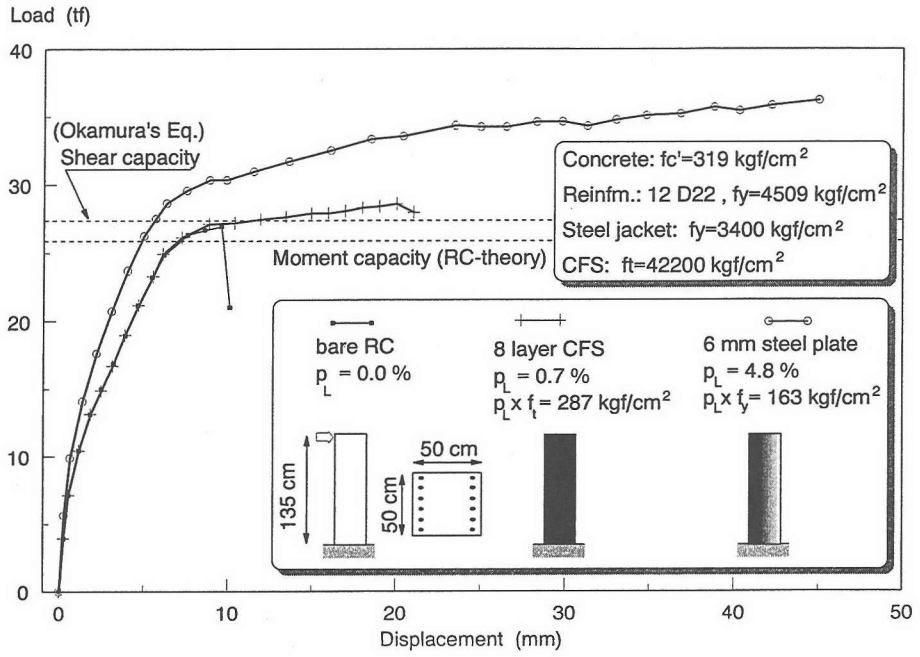

Fig.32 RC-column with similar moment and shear capacity post-strengthened by steel casing or CFS wrapping.

(1) RC-column with similar shear and moment capacity

First, an RC-column, as above (**Fig. 18**) has already been investigated. This column has moment and shear capacity very close together. Moment capacity is predicted by RC-theory whilst empirical design equation for shear strength of reinforced concrete beams without web reinforcement [21], with stirrup contribution additionally considered, is used for shear capacity estimations. In fact, it is difficult to clearly tell the failure mode in advance, since shear and moment capacity are so close to each other (**Fig.32**).

In experiment, RC-specimen failed in shear short after the yielding of main reinforcement, as was also obtained by numerical analysis. Above the same column strengthened by 6 mm steel casing was studied. Significant improvement of strength and especially ductility was obtained (**Fig. 21**).

In order to compare steel casing and CFS-wrapping, a quantity is needed not only reflecting the amount of strengthening material but also its strength. Then, lateral reinforcement ratio ρ_L is multiplied by the material strength (yield strength for steel and tensile strength for carbon fibre) that is called as equivalent amount. With ρ_L and f_y of the steel encased column and tensile strength of carbon fibre sheets given (**Fig.32**) the corresponding lateral reinforcement ratio for CFS-wrapping can be computed. In this way, five layers of fibre wrappings were determined to be nearly equivalent to 6 mm steel plate encasement. However, five layers resulted in a column response very close to the bare RC-specimen and was not plotted in **Fig.32**. In order to show some significant improvements, CFS was increased to eight layers and results are shown together with RC and steel encased specimen. From (**Fig.32**) it can be understood that, even as we provide about 1.8 times higher effective amount of CFS-wrappings steel casing still seems to be the more effective strengthening material. This might be because of the different stiffness as explained before. However, as a sufficiently high effective amount of CFS is employed, some moderate increase of ductility and strength can be obtained.

(2) RC-column failing in shear

Above, it had been shown that CFS-wrapping of an RC-column can change failure mode from brittle shear to more ductile bending failure if shear and flexural capacity are close together, but a much better performance is obtained by the equivalent amount of steel casing. Next, an RC-column that clearly fails in shear is investigated (**Fig.33**). Again it is found that if equivalent amounts of CFS are chosen similar to that of steel encased specimen response is very close to bare RC behaviour and

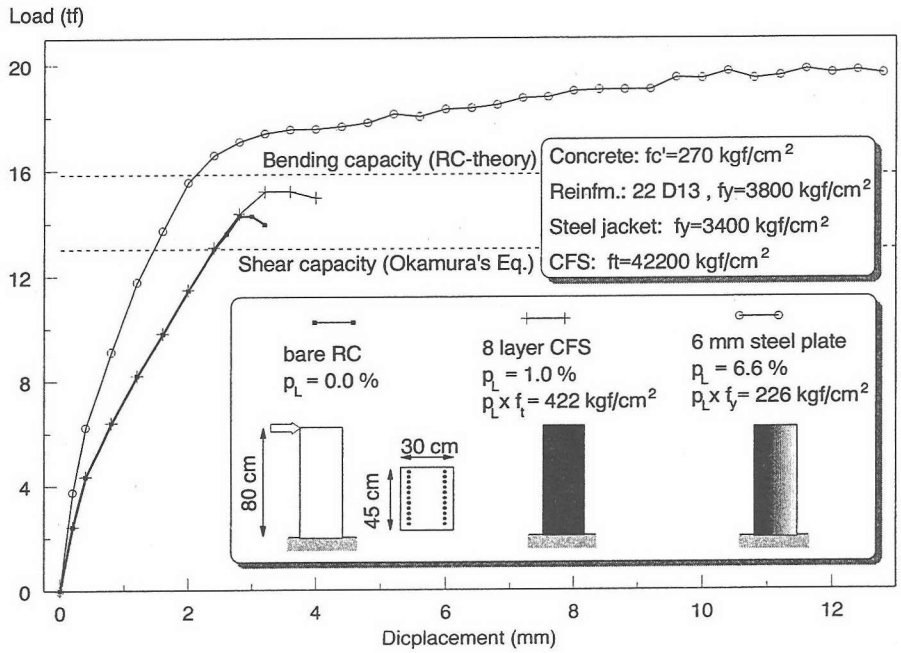

Fig.33 RC-column failing in shear post-strengthened by steel casing or CFS wrapping.

hence it is selected larger. Steel encasement largely increases shear capacity and failure mode becomes ductile flexure (**Fig.33**). For CFS-wrapping, on the other hand, even if a larger effective amount of lateral reinforcement is provided, shear failure cannot be prevented. Then, for RC-columns with shear capacity much smaller than bending capacity it seems to be preferable not to use carbon fibre sheets but steel plates for post-strengthening.

8. CONCLUSIONS

The authors seek for future possibility to make use of full-3D analytical tool for performance evaluation of strengthened RC members though the tool is no longer completed at present. For this purpose, the combination of full 3D cracked constitutive model for RC solids and softened joint interface to represent concrete/steel interface was challenged. Two strengthening materials were selected for examining the capability of 3D FEM tool since the mechanical characteristics are much different. With these materials, numerical simulations have been carried out for discussing the feasibility of 3D full analysis of strengthened systems.

Performing sectional analysis confinement performance of steel casing and CFS-wrapping was evaluated. It was found that, for steel encased columns the shear transfer mechanism between steel and concrete body strongly influences the actually induced confinement. If perfect shear transfer is assumed carbon fibre slightly outperforms steel as a confining agent. However, if the additional axial load bearing capacity, provided by steel plates with perfect shear transfer, is accounted for steel casing is more effective than CFS wrapping. Although carbon fibre exhibits very high-tension strength, due to Young's modulus similar to that of steel, the confining effect generally remains lower. Then, if CFS is to be used instead of steel for strengthening RC-columns, its high strength cannot be fully exploited and a larger available confining capacity is needed. Because of this, in practical engineering design the allowable stress in CFS shall be well below the ultimate strength.

Full structural analysis was subsequently conducted, considering more realistic steel concrete interface behaviour and the combination of bending, axial and shear forces. As column-footing joint and steel-concrete interface are considered in two separate computations, it was shown that full three-dimensional analysis of post-strengthened steel

encased RC-columns can successfully predict the load-deflection diagram up to the ductility limit. The response of RC-columns wrapped by CFS and subjected to lateral loading was also effectively predicted until the ultimate load level. However, residual post peak and residual strength as found in experiments cannot be predicted by FEM analysis. Post peak response remains essentially unsolved within the framework of the present model. The post peak compression localisation can be regarded as one of the cardinal points for a sound prediction of the descending part of the load-deflection diagram and remains a challenging topic of further research.

For RC-columns failing in flexural or shear mode, CFS wrapping brings about some moderate increase in strength and ductility. However, if steel encasement of the same equivalent amount (ρ x f) would be provided strengthening effect in terms of strength and ductility improvements are much better. If shear failure is prevailing CFS-wrapping of up to 1 % lateral reinforcement ratio brings only small strengthening effects. From the performed finite element analysis it can be concluded that when strengthening RC-columns failing in flexure, with steel encasement, special attention must be taken to maintain the rotational capacity. Possible capacity improvement due to lateral confinement induced by steel casing is contradicted by a reduced rotational capacity caused by the added axial stiffness. Then it seems that the thinner steel casing that can be provided the more effective it would be for the strengthening of RC-columns of the flexural failure mode. For RC-column failing in shear, on the other hand, a direct relationship between the amount of attached steel and strength or ductility gain was found. The more lateral steel is provided the more shear resistance might be improved and ultimately failure mode can be changed toward flexure such that higher ductility can be enjoyed.

REFERENCES

1) Knowles, R.B., and Park, R.: Axial load design for concrete filled steel tubes, *Journal of the structural division, ASCE*, Vol. 96, No. ST10, pp. 2125-2152, 1970.
2) Hajjar, J.F., and Gourley, B.C.: Representation of concrete-filled steel tube cross-section strength, *Journal of Structural Engineering*, Vol. 122, No 11, pp. 1327-1336, 1996.
3) Neogi, P.K., Sen, H.K., and Chapman, J.C.: Concrete-filled tubular steel columns under eccentric loading, *The Structural Engineer*, Vol. 47, No. 5, pp. 187-195, 1969.
4) Lu, Y.Q., and Kennedy, D.J.L: The flexural behaviour of concrete filled hollow structural sections, *Can. J. Civil Engng*, Vol. 21, No.1, pp. 111-130, 1994.
5) Hajjar, J.F., Schiller, P.H., and Molodan, A.: A distributed plasticity model for concrete-filled steel tube beam-columns with interlayer slip, *Engineering Structures*, Vol. 20, No. 8, pp. 663-676, 1998.
6) Okamura, H. and Maekawa, K.: *Nonlinear analysis and constitutive models of reinforced concrete*, Gihodo - Shuppan Co., Tokyo, 1991.
7) Hauke, B., and Maekawa, K.: Three-dimensional reinforced concrete model with multi-directional cracking, *Computational modelling of concrete structures*, Borst et al. eds., Balkema, Rotterdam and Brookfield, pp. 93-102, 1998.
8) Hauke, B., and Maekawa, K.: Generalised three-dimensional reinforced concrete post-cracking response, *Proc. of JSCE*, 1999, in preparation.
9) Maekawa, K., Takemura, J., Irawan, P. and Irie, M.: Triaxial elasto-plastic and continuum fracture model for concrete," *Concrete Library*, JSCE, No. 22, pp.131-161, 1993.
10) Maekawa, K., Irawan, P. and Okamura, H.: Path-dependent three-dimensional constitutive laws of reinforced concrete – formulation and experimental verifications, *Structural Engineering and Mechanics*, Vol. 5. No. 6, pp. 743-743, 1997.
11) An, X., Maekawa, K. and Okamura, H.: Numerical simulation of size effect in shear strength of RC beams, *J. of Materials, Concrete Structures and Pavements*, JSCE, Vol. 35, pp. 297-316, 1997.
12) Carol, I., Prat, P.C., and Lopez, C.M.: Normal/shear cracking model: application to discrete crack analysis, *Journal of Engineering Mechanics*, Vol. 123, No. 8, pp. 765-773, 1997.
13) Gao, D., Nishiumi, K., Wu. Z., and Machida, A.: Study of bond mechanism between steel plate and concrete by discontinuous FEM, *Transactions of the Japan Concrete Institute*, Vol. 17, pp. 93-98, 1995.
14) Irawan, P., and Maekawa, K.: Three-dimensional analysis of strength and deformation of confined concrete columns, *Concrete Library*, JSCE, No. 24, pp. 47-70, 1994.
15) Hosoya, M., Kawashima, K., and Hoshikuma, J.: Stress-strain relationship of concrete columns confined by carbon fibre sheets, *Tokyo Institute of Technology, Report No. 96-2*, 1996 (In Japanese).
16) Pallewatta, T.M.: *Efficiency of lateral Reinforcement on capacity of core concrete on compression,*, doctoral dissertation, The University of Tokyo, 1993.
17) Shakir-Khalil, H.: Pushout strength of concree-filled steel hollow sections, *The Structural Engineer*, Vol. 71, No. 13/6, pp. 234-233, 1993.
18) Dunberry, E., LeBlanc, D., and Redwood, R.G.: Cross-section strength of concrete-filled HSS columns at simple beam connections, *Can. J. Civil Engng*, Vol. 14, pp. 408-417, 1987.
19) Nakajima, Y., Suzuki, A., Mishima, T., and Watanabe, T.: A study for strength of reinforced concrete pier by pre-cast panel, *Proc. of JCI symposium on seismic retrofitting techniques for concrete structures*, pp. 229-236, 1997.
20) Seracino, R., Oehlers, D.J., and Yeo, M.F.: The effect of friction on the longitudinal shear force distribution along the steel-concrete interface of composite bridge beams, in Yang, Y., and Leu, L. (eds.), *Proc. of 6. East Asia-Pacific conference on structural engineering and construction*, Taipei, pp. 507-512, 1998.
21) Okamura, H., and Higai, T.: Proposed design equation for shear strength of reinforced concrete beams without web reinforcement, *Proceedings of JSCE*, 300, Aug., pp 131-141, 1980.
22) Osada, K., Ohno, S., Yamaguchi, T., and Ikeda, S.: Seismic behavior of reinforced concrete piers strengthened with carbon fibre sheets, *Concrete Library*, JSCE, No. 30, pp. 155-179, 1997.

23) Hauke, B: *Three-dimensional modelling and analysis of reinforced concrete and concrete composites*, PhD-thesis, The University of Tokyo, 1998.
24) Hauke, B., and Maekawa, K.: Strengthening of RC columns – a three-dimensional computational approach in Yang, Y., and Leu, L. (eds.), *Proc. of 6. East Asia-Pacific conference on structural engineering and construction*, Taipei, pp. 2105-2110, 1998.

(Received December 17, 1998)

後補強されたRC構造の性能評価に向けた3次元有限要素解析の応用

ベルンハルト ハウケ・前川宏一

本研究は，構造一般を対象とする数値解析手法を，鉄板および炭素繊維で補強されたRC柱の性能評価に応用する方法について，検討したものである．ひび割れを考慮した3次元RC構成モデル，炭素繊維シート，構造用鋼材，ならびに鋼材-コンクリートの境界特性モデルを有限要素解析に組み込むことで，補強された構造挙動を解析する方法を提案した．軸力，曲げ，せん断を受ける無補強および補強構造の挙動と解析結果との比較を通じて適用性と問題点を論じている．併せて，鋼材と繊維両者補強効果に差が現れる機構について，3次元解析結果から検討を加えた．